Appl. Math. Mech. -Engl. Ed., **36**(11), 1403–1416 (2015)
DOI 10.1007/s10483-015-1991-7

Applied Mathematics and Mechanics (English Edition)

Forced response of quadratic nonlinear oscillator: comparison of various approaches*

Wenan JIANG[1], Guoce ZHANG[2], Liqun CHEN[1,2,3,†]

1. Shanghai Institute of Applied Mathematics and Mechanics, Shanghai University, Shanghai 200072, China;
2. College of Sciences, Shanghai University, Shanghai 200444, China;
3. Shanghai Key Laboratory of Mechanics in Energy Engineering, Shanghai University, Shanghai 200072, China

Abstract The primary resonances of a quadratic nonlinear system under weak and strong external excitations are investigated with the emphasis on the comparison of different analytical approximate approaches. The forced vibration of snap-through mechanism is treated as a quadratic nonlinear oscillator. The Lindstedt-Poincaré method, the multiple-scale method, the averaging method, and the harmonic balance method are used to determine the amplitude-frequency response relationships of the steady-state responses. It is demonstrated that the zeroth-order harmonic components should be accounted in the application of the harmonic balance method. The analytical approximations are compared with the numerical integrations in terms of the frequency response curves and the phase portraits. Supported by the numerical results, the harmonic balance method predicts that the quadratic nonlinearity bends the frequency response curves to the left. If the excitation amplitude is a second-order small quantity of the bookkeeping parameter, the steady-state responses predicted by the second-order approximation of the Lindstedt-Poincaré method and the multiple-scale method agree qualitatively with the numerical results. It is demonstrated that the quadratic nonlinear system implies softening type nonlinearity for any quadratic nonlinear coefficients.

Key words forced vibration, quadratic nonlinearity, primary resonance, multiple-scale method, Lindstedt-Poincaré method, averaging method, harmonic balance method

Chinese Library Classification O324, O316
2010 Mathematics Subject Classification 70K50

1 Introduction

Quadratic nonlinearity arises in different models, e.g., cutting chatter[1], buckled beams[2], pneumatic systems[3], and elastic foundations[4]. A quadratic nonlinear oscillator is a useful test model for approximate analytical approaches. Therefore, the analysis on a quadratic nonlinear oscillator is a fundamental and significant subject.

* Received May 13, 2014 / Revised Sept. 5, 2014
Project supported by the State Key Program of National Natural Science Foundation of China (No. 11232009) and the National Natural Science Foundation of China (No. 11572182)
† Corresponding author, E-mail: lqchen@staff.shu.edu.cn

There are many important investigations on quadratic nonlinear oscillators. Cheung et al.[5] developed a modified Lindstedt-Poincaré method to calculate the perturbation solution of the free vibration oscillators of quadratic nonlinearity, and demonstrated that the results were in excellent agreement with those obtained by the incremental harmonic balance method. Huseyin and Lin[6] used an intrinsic multiple-scale harmonic balance technique to study the approximate solutions of free quadratic and cubic nonlinear oscillators. Xu and Cheung[7] employed the averaging method based on the generalized harmonic functions to seek the approximate solutions of strongly nonlinear oscillators, and supported the resulting solutions by the numerical integration. Pakdemirli[8] used the multiple-scale method to investigate the continuous free vibration systems with quadratic and cubic nonlinearities. Chen et al. proposed the elliptic perturbation method[9] and the elliptic Lindstedt-Poincaré method[10] to determine the periodic solution of the free vibration of quadratic nonlinear oscillators, and found that the solution obtained by the elliptic perturbation method was more accurate than that obtained by the Lindstedt-Poincaré method. Lakrad and Belhaq[11] employed the multiple-scale method with the Jacobian elliptic functions to calculate the solution of nonlinear quadratic and cubic self-excited systems. Mickens[12] used the phase space techniques to compare the free vibrations of three types of quadratic nonlinear oscillators. Cveticanin[13] utilized the Jacobian elliptic function to express the exact analytical solution of a mass-spring oscillator with strong quadratic nonlinearity. Wu and Lim[14] combined the harmonic balance method and the linearization to construct the approximate analytical solutions of a conservative quadratic nonlinear oscillator, and showed that the obtained solutions were in good agreement with the exact solutions. Hu[15–17] conducted a systematic investigation on the conservative quadratic nonlinear oscillator, expressed the exact solution of the oscillator in the Jacobian elliptic function[15], proposed a modified iteration scheme with a higher accuracy than the first-order harmonic balance method[16], and demonstrated that the harmonic balance method was more accurate than the second approximate solution of the Lindstedt-Poincaré method[17]. It should be remarked that the harmonic balance method[17] is without the zeroth-order harmonic component.

All the above-mentioned works on quadratic nonlinear oscillators focus on the free vibration without external excitations. There are no investigations on the forced vibration of quadratic nonlinear oscillators, even in the case of weak nonlinearity. To address the lack of research in the aspect, the present work treats the primary resonance of quadratic nonlinear oscillators. Interestingly, various approximate analytical approaches yield different quantitatively and qualitatively results.

The manuscript is organized as follows. Section 2 introduces a quadratic nonlinear oscillator as the truncated model of the snap-through mechanism. Section 3 treats the forced quadratic nonlinear oscillators by use of the Lindstedt-Poincaré method, the multiple-scale method, the averaging method, and the harmonic balance method. Section 4 compares the analytical outcomes with the numerical calculations. Section 5 ends the paper with concluding remarks.

2 Snap-through mechanism as quadratic nonlinear oscillator

The research relevant to the snap-through mechanism can be dated back to Thompson and Hunt[18]. Recently, the possibility of the application of the device in harvesting vibration energy was explored[19]. Figure 1 shows the snap-through mechanism under a base excitation. The dynamic equation can be derived from the Newton law as follows:

$$m\ddot{x}+c\dot{x}+2k_{\mathrm{s}}\Big(1-\frac{L}{\sqrt{x^2+l^2}}\Big)x+mg=-m\ddot{y}, \tag{1}$$

where m is the mass, x is the displacement of the mass, c is the damping coefficient, k_{s} is the spring stiffness, L is the original length of the spring, l is the distance between the center and the edge of the frame, θ is the inclination of the spring with respect to the horizontal, g is the gravitational acceleration, and y is a harmonic base excitation.

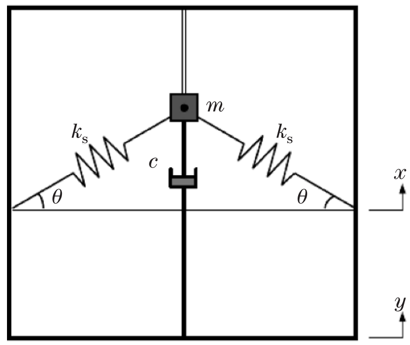

Fig. 1 Device of mass-spring-damper for snap-through mechanism

The static equilibrium positions of the system satisfy the equation as follows:

$$2k_{\rm s}\Big(1-\frac{L}{\sqrt{x^2+l^2}}\Big)x+mg=0. \tag{2}$$

For the excited small-amplitude motion, the snap-through system undergoes a motion around an equilibrium point. In this case, the nonlinear term in (1) can be expanded into the Taylor series at a stable equilibrium $(x_1,\ 0)$ solved by (2). Omitting the higher order terms in the resulting expanding expression and shifting the origin of the coordinate by introducing the new variable $x \leftrightarrow x - x_1$, one can cast (1) into the dimensionless form as follows:

$$\ddot{x}+\varepsilon c\dot{x}+\omega^2 x+\varepsilon\alpha x^2=\varepsilon f\cos(\Omega t) \tag{3}$$

for small base excitation, where x is the dimensionless generalized coordinate, ε is a small parameter, c is a damping coefficient, ω is the natural frequency, α is the coefficient of the quadratic nonlinear term, and f and Ω are the amplitude and the frequency of the harmonic force, respectively.

In the following, the primary resonance is treated. In this case, the excitation frequency is very close to the natural frequency. Introduce the detuning parameter σ_0 satisfying

$$\Omega=\omega+\varepsilon\sigma_0. \tag{4}$$

3 Analytical approximation of amplitude-frequency relationship

3.1 Lindstedt-Poincaré method

The Lindstedt-Poincaré method assumes an approximate expansion of the solution of (3) in the form as follows:

$$x(t,\varepsilon)=x_0+\varepsilon x_1+\cdots. \tag{5}$$

Substituting (4) and (5) into (3) and equating the coefficients of the same order ε yield

$$x_0''+x_0=0, \tag{6}$$

$$x_1''+x_1=-\frac{2\sigma_0}{\omega}x_0''-\frac{c}{\omega}x_0'-\frac{\alpha}{\omega^2}x_0^2+\frac{f}{\omega^2}\cos\tau, \tag{7}$$

where x' represents the derivative of x with respect to the new time scale $\tau=\Omega t$.

The solution of (6) is

$$x_0 = a\cos(\tau + \varphi) \tag{8}$$

with the amplitude a and the initial phase φ. Substituting (8) into (7) and eliminating the secular terms lead to

$$\frac{2\sigma_0}{\omega}a + \frac{f}{\omega^2}\cos\varphi = 0, \quad \frac{c}{\omega}a + \frac{f}{\omega^2}\sin\varphi = 0. \tag{9}$$

Eliminating φ from (9), we can obtain the amplitude-frequency response relationship as follows:

$$a = \frac{f}{\omega\sqrt{4\sigma_0^2 + c^2}}, \tag{10}$$

which is actually the amplitude-frequency response relationship of a linear oscillator defined by (3) where $\alpha = 0$. Therefore, up to the first-order approximation, the Lindstedt-Poincaré method cannot account for the quadratic nonlinearity.

Substituting (8) into (7) and omitting the secular terms yield

$$x_1 = -\frac{\alpha a^2}{2\omega^2} + \frac{\alpha a^2}{6\omega^2}\cos(2(\tau + \varphi)). \tag{11}$$

According to (5), we can obtain the second-order approximation as follows:

$$x(t, \varepsilon) = -\frac{\varepsilon\alpha a^2}{2\omega^2} + a\cos(\tau + \varphi) + \frac{\varepsilon\alpha a^2}{6\omega^2}\cos 2(\tau + \varphi), \tag{12}$$

indicating that the amplitude of the second-order approximation comes from the first-order approximation. However, the amplitude-frequency response relationship of the first-order approximation is linear. Consequently, when the excitation amplitude is a first-order small quantity of the bookkeeping parameter, the second-order approximation does not have multivaluedness and bending.

3.2 Multiple-scale method

The multiple-scale method assumes an approximate expansion of the solution of (3) in the following form:

$$x(t, \varepsilon) = x_0(T_0, T_1) + \varepsilon x_1(T_0, T_1) + \cdots, \tag{13}$$

where

$$T_0 = t, \quad T_1 = \varepsilon t.$$

Denote

$$D_k = \frac{\partial}{\partial T_k}, \quad k = 0, 1.$$

Then,

$$\frac{\mathrm{d}}{\mathrm{d}t} = D_0 + \varepsilon D_1 + \cdots, \quad \frac{\mathrm{d}^2}{\mathrm{d}t^2} = D_0^2 + 2\varepsilon D_0 D_1 + \cdots. \tag{14}$$

Substituting (13) and (14) into (3) and equating the coefficients of ε^0 and ε^1 yield

$$D_0^2 x_0 + \omega^2 x_0 = 0, \tag{15}$$

$$D_0^2 x_1 + \omega^2 x_1 = -2D_0 D_1 x_0 - cD_0 x_0 - \alpha x_0^2 + f\cos(\Omega T_0). \tag{16}$$

The solution of (15) can be expressed as follows:

$$x_0 = A(T_1)\exp(\mathrm{i}\omega T_0) + \text{c.c.}, \tag{17}$$

where $A(T_1)$ is an unknown complex function of T_1, and c.c. stands for the complex conjugate of the preceding terms. Substituting (17) into (16) and eliminating the secular terms yield

$$-2\mathrm{i}\omega D_1 A - \mathrm{i}\omega A c + \frac{f}{2}\exp(\mathrm{i}\sigma_0 T_1) = 0. \tag{18}$$

Express the unknown function A in the polar form as follows:

$$A(T_1) = \frac{1}{2}a(T_1)\exp(\mathrm{i}\theta(T_1)). \tag{19}$$

Substituting (19) into (18) and separating the resulting equation into real and imaginary parts, one has

$$\frac{\mathrm{d}a}{\mathrm{d}T_1} = -\frac{ca}{2} + \frac{f}{2\omega}\sin\gamma, \quad a\frac{\mathrm{d}\gamma}{\mathrm{d}T_1} = a\sigma_0 + \frac{f}{2\omega}\cos\gamma, \tag{20}$$

where

$$\gamma = \sigma_0 T_1 - \theta.$$

For a steady-state response, both a and γ should be constants. Therefore, from (20), we get

$$-\frac{ca}{2} + \frac{f}{2\omega}\sin\gamma = 0, \quad a\sigma_0 + \frac{f}{2\omega}\cos\gamma = 0. \tag{21}$$

Eliminating γ from (21) yields (10). Thus, the amplitude-frequency response relationship derived from the multiple-scale method is the same as that derived from the Lindstedt-Poincaré method.

Substituting (19) into (17) and omitting the secular terms yield

$$x_1 = -\frac{2\alpha A\bar{A}}{\omega^2} + \frac{\alpha A^2}{3\omega^2}\exp(\mathrm{i}2\omega T_0). \tag{22}$$

Substituting (17) and (22) into (13) yields the second approximate as follows:

$$x(t,\varepsilon) = -\frac{\varepsilon\alpha a^2}{2\omega^2} + \frac{a}{2}\exp(\mathrm{i}\,(\theta(T_1) + \omega T_0)) + \frac{\varepsilon\alpha a^2}{12\omega^2}\exp(2\mathrm{i}(\theta(T_1) + \omega T_0)). \tag{23}$$

Thus, the second approximate derived from the multiple-scale method is the same as that derived from the Lindstedt-Poincaré method.

3.3 Averaging method

The averaging method is employed to seek the solution to (3) in the form as follows:

$$\ddot{x} + \Omega^2 x = \varepsilon F(x, \dot{x}, \Omega t), \tag{24}$$

where

$$F(x, \dot{x}, \Omega t) = 2\sigma_0\omega x - \alpha x^2 - c\dot{x} + f\cos(\Omega t). \tag{25}$$

The averaging method assumes the solution of (24) in the following form:

$$x = a(\varepsilon t)\cos(\Omega t - \varphi(\varepsilon t)), \quad \dot{x} = -\Omega a(\varepsilon t)\sin(\Omega t - \varphi(\varepsilon t)). \tag{26}$$

Let $\psi = \Omega t - \varphi$. Then, (24) and (26) yield

$$\begin{cases} \dot{a} = -\dfrac{\varepsilon}{\Omega}F(a\cos\psi, -\Omega a\sin\psi, \psi + \varphi)\sin\psi, \\ a\dot{\varphi} = F(a\cos\psi, -\Omega a\sin\psi, \psi + \varphi)\cos\psi. \end{cases} \tag{27}$$

Averaging the right-hand sides of (27) over ψ from 0 to 2π yields

$$\begin{cases} \dot{a} = -\dfrac{\varepsilon}{\Omega}\dfrac{1}{2\pi}\displaystyle\int_0^{2\pi} F(a\cos\psi, -\Omega a\sin\psi, \psi+\varphi)\sin\psi \mathrm{d}\psi, \\ a\dot{\varphi} = \dfrac{\varepsilon}{\Omega}\dfrac{1}{2\pi}\displaystyle\int_0^{2\pi} F(a\cos\psi, -\Omega a\sin\psi, \psi+\varphi)\cos\psi \mathrm{d}\psi. \end{cases} \tag{28}$$

Substituting (25) into (28) yields

$$\begin{cases} \dot{a} = -\dfrac{\varepsilon}{2\Omega}\left(ca\Omega - f\sin\varphi\right), \\ a\dot{\varphi} = \dfrac{\varepsilon}{2\Omega}\left(2\sigma_0 a\omega + f\cos\varphi\right). \end{cases} \tag{29}$$

For a steady-state response, both a and φ should be constants. Therefore,

$$-\frac{\varepsilon}{2\Omega}\left(ca\Omega - f\sin\varphi\right) = 0, \quad \frac{\varepsilon}{2\Omega}\left(2\sigma_0 a\omega + f\cos\varphi\right) = 0. \tag{30}$$

Eliminating φ from (30) yields the amplitude-frequency response relationship as follows:

$$a = \frac{f}{\omega\sqrt{4\sigma_0^2 + c^2\frac{\Omega^2}{\omega^2}}}. \tag{31}$$

(10) and (31) indicate that the amplitude-frequency response relationship derived from the averaging method is not identical to that obtained by the Lindstedt-Poincaré method or the multiple-scale method.

3.4 Harmonic balance method

The harmonic balance method assumes that the solution of (3) is

$$x = a_0 + a_1\cos(\Omega t) + b_1\sin(\Omega t), \tag{32}$$

where a_0, a_1, and b_1 are the coefficients to be determined.

Substituting (32) into (3) and equalizing the coefficients of the constant terms and the first harmonic components yield

$$\begin{cases} \omega^2 a_0 + \varepsilon\alpha a_0^2 + \dfrac{\varepsilon\alpha}{2}a_1^2 + \dfrac{\varepsilon\alpha}{2}b_1^2 = 0, \\ \left(\omega^2 - \Omega^2\right)b_1 - \varepsilon c\Omega a_1 + 2\varepsilon\alpha a_0 b_1 = 0, \\ \left(\omega^2 - \Omega^2\right)a_1 + \varepsilon c\Omega b_1 + 2\varepsilon\alpha a_0 a_1 = \varepsilon f. \end{cases} \tag{33}$$

Decoupling a_0 from a_1 and b_1 in (33) yields

$$\begin{aligned} &8\varepsilon^3\alpha^3 a_0^4 + 8\varepsilon^2\alpha^2(2\omega^2 - \Omega^2)a_0^3 + 2\varepsilon\alpha\left((\omega^2-\Omega^2)(5\omega^2-\Omega^2) + \varepsilon^2 c^2\Omega^2\right)a_0^2 \\ &+2\omega^2\left((\omega^2-\Omega^2)^2 + (\varepsilon c\Omega)^2\right)a_0 + \varepsilon^3\alpha f^2 = 0. \end{aligned} \tag{34}$$

Once a_0 has been determined, a_1 and b_1 can be solved as follows:

$$\begin{cases} a_1 = \dfrac{\left(-\Omega^2 + \omega^2 + 2\varepsilon\alpha a_0\right)\varepsilon f}{\left(-\Omega^2 + \omega^2 + 2\varepsilon\alpha a_0\right)^2 + \left(\varepsilon c\Omega\right)^2}, \\ b_1 = \dfrac{\varepsilon^2 c\Omega f}{\left(-\Omega^2 + \omega^2 + 2\varepsilon\alpha a_0\right)^2 + \left(\varepsilon c\Omega\right)^2}. \end{cases} \tag{35}$$

Then, the amplitude-frequency response relationship can be calculated by

$$a = |a_0| + \sqrt{a_1^2 + b_1^2}. \tag{36}$$

3.5 Three-time scale method

We seek a solution of (3) in the three time scales form

$$x(t,\varepsilon)=x_0(T_0,T_1,T_2)+\varepsilon x_1(T_0,T_1,T_2)+\varepsilon^2x_2(T_0,T_1,T_2)+\cdots, \tag{37}$$

where

$$T_k=\varepsilon^k t,\quad k=0,1,2.$$

Denote

$$D_k=\frac{\partial}{\partial T_k},\quad k=0,1,2.$$

Then,

$$\frac{\mathrm{d}}{\mathrm{d}t}=D_0+\varepsilon D_1+\varepsilon^2D_2+\cdots,\quad \frac{\mathrm{d}^2}{\mathrm{d}t^2}=D_0^2+2\varepsilon D_0D_1+\varepsilon^2(D_1^2+2D_0D_2)+\cdots. \tag{38}$$

Use the three-time scale method to rescale the damping coefficient, the amplitude of excitation, and the detuning parameter, respectively, i.e.,

$$c\leftrightarrow\varepsilon c,\quad f\leftrightarrow\varepsilon f,\quad \Omega=\omega+\varepsilon^2\sigma_0. \tag{39}$$

Then, we can rewrite the equation of the system as follows:

$$\ddot{x}+\varepsilon^2c\dot{x}+\omega^2x+\varepsilon\alpha x^2=\varepsilon^2f\cos(\Omega t). \tag{40}$$

Substituting (37), (38), and (39) into (40) and equating the coefficients of the same power ε yield

$$D_0^2x_0+\omega^2x_0=0, \tag{41}$$

$$D_0^2x_1+\omega^2x_1=-2D_0D_1x_0-\alpha x_0^2, \tag{42}$$

$$D_0^2x_2+\omega^2x_2=-2D_0D_1x_1-cD_0x_0-(D_1^2+2D_0D_2)x_0-2\alpha x_0x_1+f\cos(\Omega T_0). \tag{43}$$

The solution of (41) can be expressed as follows:

$$x_0(T_0,T_1,T_2)=A(T_1,T_2)\exp(\mathrm{i}\omega T_0)+\mathrm{c.c.} \tag{44}$$

Substituting (44) into (42) and eliminating the secular terms yield

$$D_1A=0\Rightarrow A=A(T_2). \tag{45}$$

With this result, the solution of (42) can be written as follows:

$$x_1\left(T_0,T_2\right)=\frac{\alpha}{3\omega^2}A^2\left(T_2\right)\exp(2\mathrm{i}\omega T_0)-\frac{2\alpha}{\omega^2}A\left(T_2\right)\bar{A}\left(T_2\right)+\mathrm{c.c.} \tag{46}$$

Substituting (44) and (46) into (43) and eliminating the secular terms yield

$$-\mathrm{i}c\omega A-2\mathrm{i}\omega D_2A+\frac{10\alpha^2}{3\omega^2}A^2\bar{A}+\frac{1}{2}f\mathrm{e}^{\mathrm{i}\sigma_0T_2}=0. \tag{47}$$

Express the unknown function A in the polar form as follows:

$$A(T_2)=\frac{1}{2}a(T_2)\exp(\mathrm{i}\theta(T_2)). \tag{48}$$

Substituting (48) into (47) and separating the resulting equation into real and imaginary parts yield

$$\frac{\mathrm{d}a}{\mathrm{d}T_2} = -\frac{ca}{2} + \frac{f}{2\omega}\sin\gamma, \quad a\frac{\mathrm{d}\gamma}{\mathrm{d}T_2} = a\sigma_0 + \frac{5\alpha^2}{12\omega^2}a^3 + \frac{f}{2\omega}\cos\gamma, \tag{49}$$

where

$$\gamma = \sigma_0 T_2 - \theta.$$

For a steady-state response, both a and γ should be constants. Therefore, (49) leads to

$$-\frac{ca}{2} + \frac{f}{2\omega}\sin\gamma = 0, \quad a\sigma_0 + \frac{5\alpha^2}{12\omega^2}a^3 + \frac{f}{2\omega}\cos\gamma = 0. \tag{50}$$

Eliminating γ from (50) yields the amplitude-frequency response relationship derived from the three-time scale method as follows:

$$\sigma_0 = -\frac{5\alpha^2}{12\omega^3}a^2 \pm \frac{1}{2\omega a}\sqrt{f^2 - c^2\omega^2 a^2}, \tag{51}$$

where the characteristic of nonlinearity exists.

The amplitude of (50) satisfies the following condition:

$$a \leqslant \frac{f}{c\omega}. \tag{52}$$

When the amplitude of the steady-state response is the maximum, the detuning parameter is

$$\sigma* = -\frac{5\alpha^2 f^2}{12c^2\omega^5}. \tag{53}$$

It should be noticed that the detuning is negative for any quadratic nonlinear coefficients. Therefore, the quadratic nonlinear system results in the softening type nonlinear characteristic.

Substituting (48) into (44) and (46), according to (37), we can obtain the second-order approximate as follows:

$$\begin{aligned} x\left(t,\varepsilon\right) &= x_0\left(T_0,T_1,T_2\right) + \varepsilon x_1\left(T_0,T_1,T_2\right) + \cdots \\ &= a\cos\left(\omega t+\theta\right) - \frac{\varepsilon\alpha a^2}{2\omega^2} + \frac{\varepsilon\alpha a^2}{6\omega^2}\cos\left(2\omega t + 2\theta\right) + O\left(\varepsilon^2 a^2\right). \end{aligned} \tag{54}$$

Using the same scale, the second-order approximation derived from the Lindstedt-Poincaré method is the same as that derived from the three-time scale method.

Although the form of (54) is the same as (12) and (23), the amplitude of (54) comes from the amplitude-frequency response relationship (51) which is nonlinear. Consequently, the second-order approximation of the three-time scale method has multivaluedness and bending. Therefore, the three-time scale method can predict the steady-state response of the quadratic nonlinear system.

3.6 Primary resonance under strong harmonic excitation

Now, consider a quadratic nonlinearity oscillator subject to a strong external harmonic excitation, i.e.,

$$\ddot{x} + \varepsilon c\dot{x} + \omega^2 x + \varepsilon\alpha x^2 = f\cos(\Omega t). \tag{55}$$

In the primary resonance, it is difficult to directly apply the Lindstedt-Poincaré method and the multiple-scale method, because the secular term occurs in the zeroth-order approximation. The averaging method still works. The similar procedure in Subsection 3.4 leads to the amplitude-frequency response relationship for (55) as follows:

$$a = \frac{f}{\varepsilon\sqrt{4\sigma_0^2\omega^2 + c^2\Omega^2}}. \tag{56}$$

The harmonic balance method is also valid. The similar procedure in Subsection 3.4 leads to the amplitude-frequency response relationship (36). Therefore, we can obtain a_0 by

$$8\varepsilon^3\alpha^3a_0^4+8\varepsilon^2\alpha^2(2\omega^2-\Omega^2)a_0^3+2\varepsilon\alpha\left((\omega^2-\Omega^2)(5\omega^2-\Omega^2)+\varepsilon^2c^2\Omega^2\right)a_0^2$$
$$+2\omega^2\left((\omega^2-\Omega^2)^2+(\varepsilon c\Omega)^2\right)a_0+\varepsilon\alpha f^2=0 \tag{57}$$

and a_1 and b_1 by

$$\begin{cases} a_1=\dfrac{\left(-\Omega^2+\omega^2+2\varepsilon\alpha a_0\right)f}{\left(-\Omega^2+\omega^2+2\varepsilon\alpha a_0\right)^2+\left(\varepsilon c\Omega\right)^2}, \\ b_1=\dfrac{\varepsilon c\Omega f}{\left(-\Omega^2+\omega^2+2\varepsilon\alpha a_0\right)^2+\left(\varepsilon c\Omega\right)^2}. \end{cases} \tag{58}$$

4 Comparisons of numerical results

To examine the analytical results in the preceding section, the fourth-order Runge-Kutta algorithm is employed to integrate (3) and (55). The parameters are chosen as follows: $\varepsilon=0.01$, $\omega=1$, $c=2$, and $\alpha=5$.

4.1 Primary resonance under weak harmonic excitation

Figure 2 shows the amplitude-frequency response curves of (3) with (4) for two excitation amplitudes. In Fig. 2, the hollow dot lines, the solid (stable) lines, and the solid lines with solid dots stand for the outcomes of the numerical integration, the harmonic balance method, and the multiple-scale method, respectively. The outcome of the Lindstedt-Poincaré method is identical to that of the multiple-scale method, and the outcome of the averaging method is so close that there are no differences among the results in the figure. For rather small excitation amplitude shown in Fig. 2(a), all curves are qualitatively the same in the sense that the amplitude-frequency response relationships are all single-valued, while the response curve obtained by the harmonic balance method is quantitatively more close to the numerical result than to that obtained by the multiple-scale method. For relatively large excitation amplitude shown in Fig. 2(b), the outcome of the numerical integration agrees qualitatively with that of the harmonic balance method. Both the curves bend to the left, while the cubic nonlinearity with the positive coefficient bends the curve to the right. In each of the curve, there is multi-valuedness, resulting in jumping. In spite of the qualitative agreement, there are certain quantitative differences.

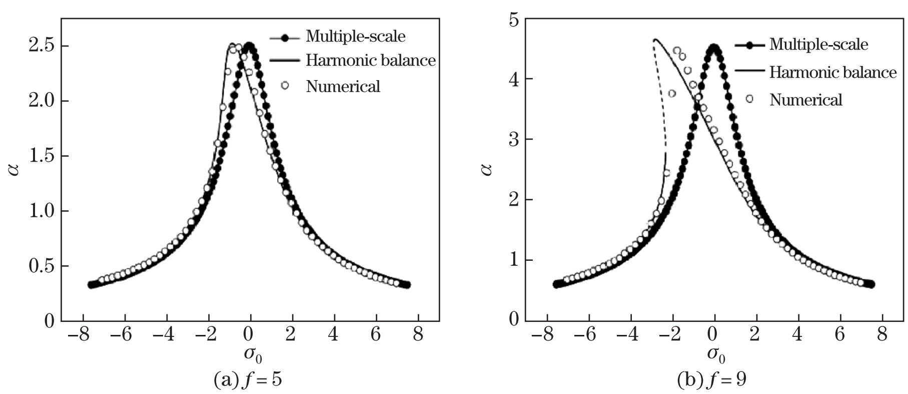

Fig. 2 Amplitude-frequency response curves for weak excitations

To highlight the quantitative differences among different approaches, the phase portraits of the steady-state responses are illustrated in Fig. 3 for a few sets of parameters. In Fig. 3, the solid dot lines, the solid lines, the dash lines, and the dash dot lines represent the results of the numerical integrations, the harmonic balance method, the multiple-scale method (also the Lindstedt-Poincaré method), and the averaging method, respectively. In all cases, the results of the method of harmonic balance are the best approximations supported by the numerical results.

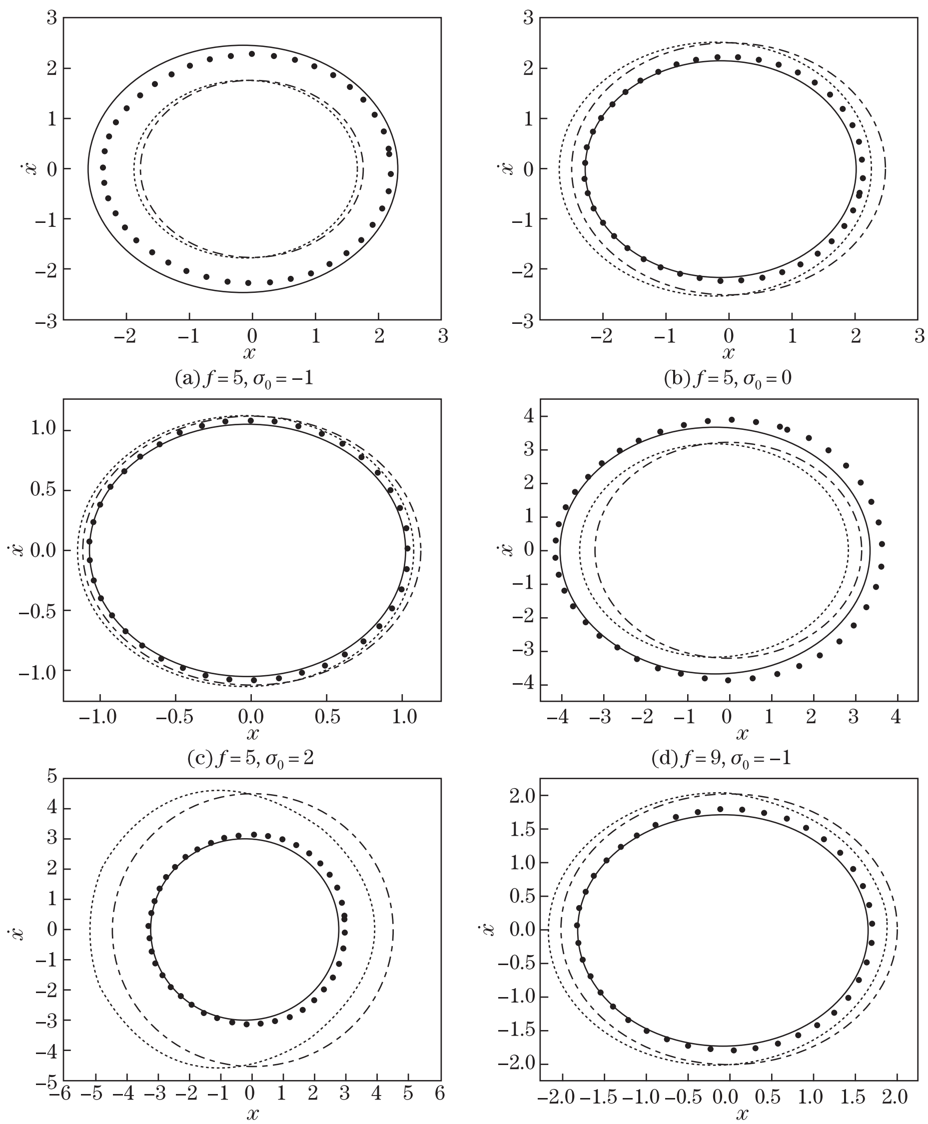

(a) $f=5$, $\sigma_0=-1$ (b) $f=5$, $\sigma_0=0$

(c) $f=5$, $\sigma_0=2$ (d) $f=9$, $\sigma_0=-1$

(e) $f=9$, $\sigma_0=0$ (f) $f=9$, $\sigma_0=2$

Fig. 3 Phase portraits of steady-state responses to weak excitations for different parameters

Figure 4 depicts the amplitude-frequency response curves of the second-order approximation derived from the two-time scale method. The outcome of the Lindstedt-Poincaré method under the same scale is identical to those of the two-time scale method. In Fig. 4, the solid triangles are the numerical results based on the original (1), the hollow dot lines are the numerical results based on the truncated (3), and the solid and dashed lines stand for the results of the second approximate and the first approximate of the two-time scale method, respectively. The numerical solutions of (1) and (3) are demonstrated to be in good agreement. It is evident that the second-order approximation derived from the two-time scale method cannot predict any bending in the response curves.

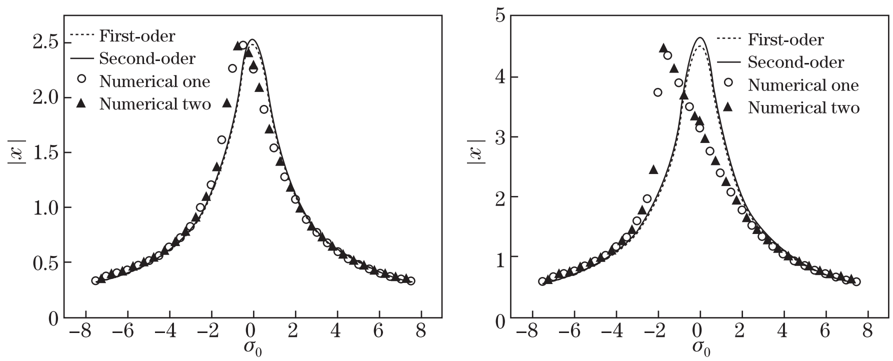

(a) $f = 5$ (b) $f = 9$

Fig. 4 Amplitude-frequency response curves under weak excitations

Figure 5 shows the amplitude-frequency response curves of the second-order approximation derived from the three-time scale method, the two-time scale method, the harmonic balance method, and the numerical results, respectively. The results indicate that the second-order approximation of the three-time scale method bends to the left, agreeing qualitatively with the numerical observations. The simulations and theoretical analyses reveal that the harmonic balance method can outperform the averaging method, the Lindstedt-Poincaré method, and the multiple-scale method for the quadratic nonlinear system under weak external excitations.

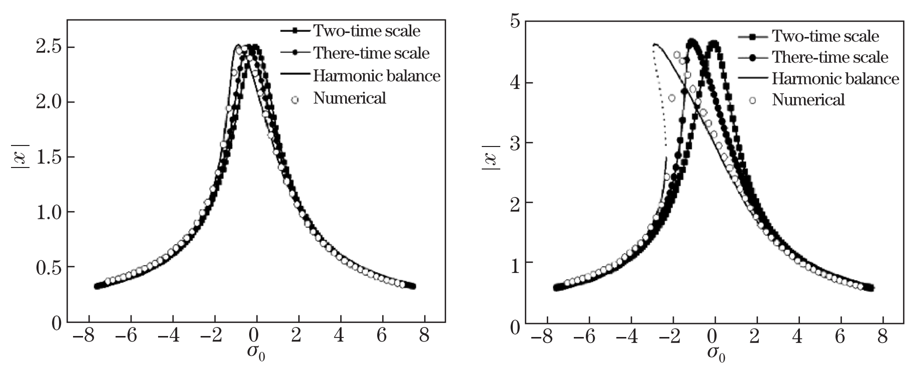

(a) $f = 5$ (b) $f = 9$

Fig. 5 Amplitude-frequency response curves under weak excitations

4.2 Primary resonance under a strong harmonic excitation

Figure 6 depicts the amplitude-frequency response curves of (55) with (4) determined by the numerical integration (hollow dot lines), the harmonic balance method (solid lines for stable portions and dashed lines for unstable portions), and the averaging method (solid lines with solid dots). The averaging method cannot reveal the effect of quadratic nonlinearity, since the resulting response curves are without bending. The harmonic balance method predicts bending of the response curves to the left, and the prediction is supported by the numerical results. For the quadratic nonlinear term with negative coefficients, the only change made by the transform $x \leftrightarrow -x$ is the sign of the forcing term in the resulting governing equation. According to (36), (57), and (58), the forcing term sign change does alter the amplitude-frequency response relationship. Contrast to the cubic nonlinearity, the quadratic nonlinearity, regardless its coefficient sign, bends the response curves to the left instead of the right.

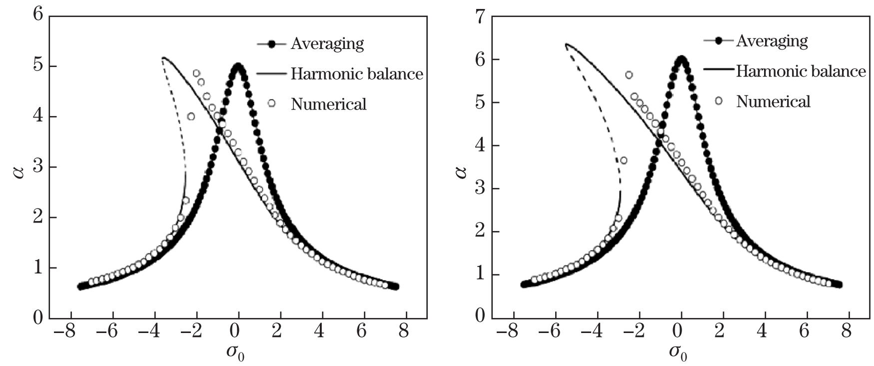

(a) $f = 5$ (b) $f = 9$

Fig. 6 Frequency response curve under different excitations

For a few sets of parameters, Fig. 7 plots the phase portraits of the steady-state responses determined by the numerical integration (solid dot lines), the harmonic balance method (solid lines), and the averaging method (dashed lines). The quantitative differences between the results of the numerical integration and the harmonic balance method are rather small.

5 Conclusions

The present work analyzes the steady-state response in the primary resonance of a quadraticly nonlinear oscillator subject to weak external excitations and strong external excitations. The analytical approximations of the amplitude-frequency response relationships are derived from the Lindstedt-Poincaré method, the multiple-scale method , the averaging method, and the harmonic balance method. The analytical results are compared with the numerical integrations. The investigation yields the following conclusions:

(i) The harmonic balance method reveals that the quadratic nonlinearity bends the amplitude-frequency response curves to the left.

(ii) The left-bending predicted by the harmonic balance method is supported by the numerical integrations.

(iii) Up to the first-order approximation, the Lindstedt-Poincaré method, the multiple-scale method, and the averaging method cannot account for the quadratic nonlinearity, and thus cannot predict any bending in the amplitude-frequency response curves.

(iv) It is demonstrated that there exists a zeroth-order harmonic component in the application of the harmonic balance method to the forced quadratic nonlinearity oscillator.

(v) Up to the second-order approximation, the two-time scale method cannot predict any bending in the response curves, while the three-time scale method can predict any bending.

(vi) Simulations and theoretical analyses reveal that the harmonic balance method can outperform the averaging method, the Lindstedt-Poincaré method, and the multiple-scale method for the quadratic nonlinear system under weak external excitations.

(vii) It is also demonstrated that the quadraticly nonlinear system indicates a softening type nonlinearity for any quadratic nonlinear coefficients.

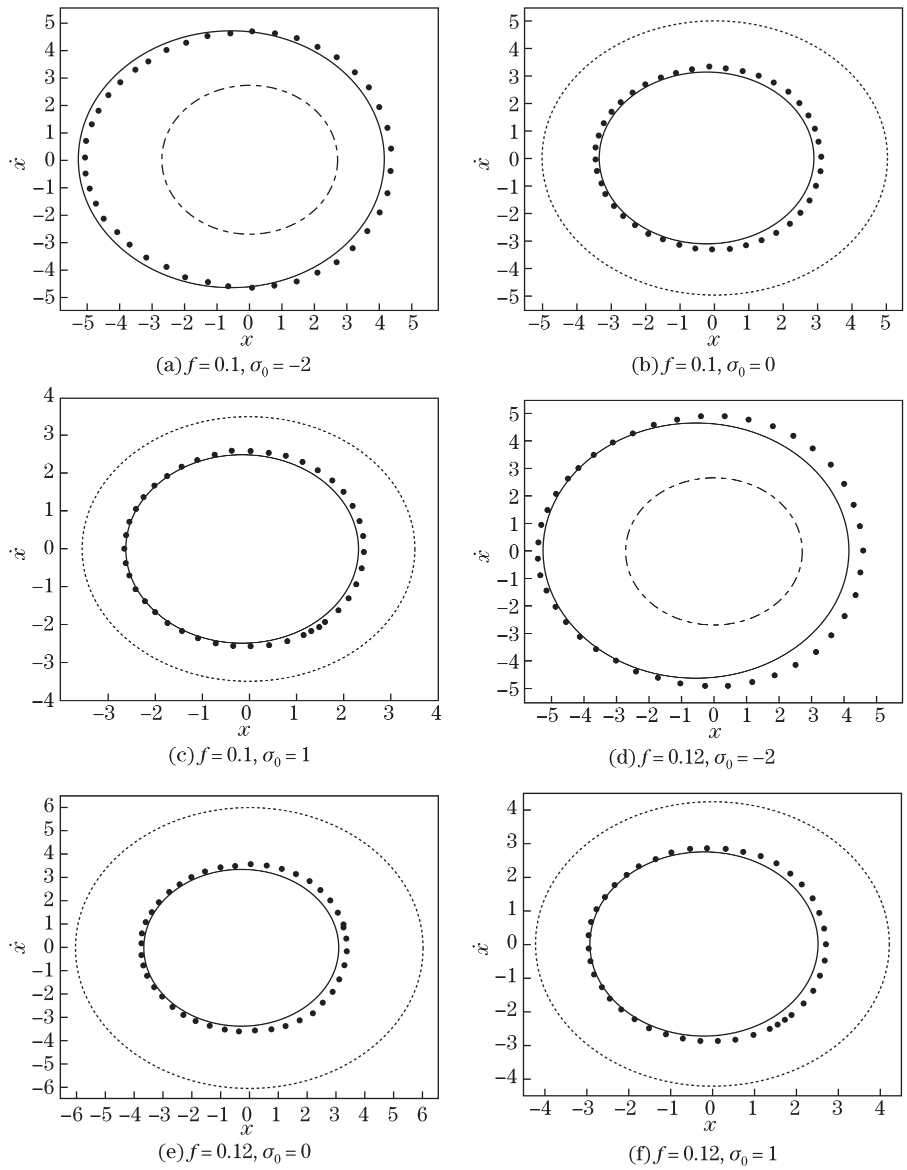

Fig. 7 Phase portraits of steady-state responses under strong excitations with different parameters

References

[1] Hanna, N. and Tobias, S. A theory of nonlinear regenerative chatter. *Journal of Manufacturing Science and Engineering*, **96**, 247–255 (1974)

[2] Abou-Rayan, A. M., Nayfeh, A. H., Mook, D. T., and Nayfeh, M. A. Nonlinear responses of a parametrically excited buckled beam. *Nonlinear Dynamics*, **4**, 499–525 (1993)

[3] Nayfeh, A. H., Nayefeh, J. F., and Mook, D. T. On methods for continuous systems with quadratic and cubic nonlinearities. *Nonlinear Dynamics*, **3**, 145–162 (1992)

[4] Nayfeh, A. H. and Lacarbonara, W. On the discretization of distributed-parameter systems with quadratic and cubic nonlinearities. *Nonlinear Dynamics*, **13**, 203–220 (1997)

[5] Cheung, Y. K., Chen, S. H., and Lau, S. L. A modified Lindstedt-Poincaré method for certain

strongly nonlinear oscillators. *International Journal of Non-Linear Mechanics*, **26**, 367–378 (1991)

[6] Huseyin, K. and Lin, R. An intrinsic multiple-scale harmonic-balance method for nonlinear vibration and bifurcation problems. *International Journal of Non-Linear Mechanics*, **26**, 727–740 (1991)

[7] Xu, Z. and Cheung, Y. K. Averaging method using generalized harmonic functions for strongly nonlinear oscillators. *Journal of Sound and Vibration*, **174**, 563–576 (1994)

[8] Pakdemirli, M. A comparison of two perturbation methods for vibrations of systems with quadratic and cubic nonlinearities. *Mechanics Research Communications*, **21**, 203–208 (1994)

[9] Chen, S. H., Yang, X. M., and Cheung, Y. K. Periodic solutions of strongly quadratic nonlinear oscillators by the elliptic perturbation method. *Journal of Sound and Vibration*, **212**, 771–780 (1998)

[10] Chen, S. H., Yang, X. M., and Cheung, Y. K. Periodic solutions of strongly quadratic nonlinear oscillators by the elliptic Lindstedt-Poincaré method. *Journal of Sound and Vibration*, **227**, 1109–1118 (1999)

[11] Lakrad, F. and Belhaq, M. Periodic solutions of strongly nonlinear oscillators by the multiple scales method. *Journal of Sound and Vibration*, **258**, 677–700 (2002)

[12] Mickens, R. E. Quadratic nonlinear oscillators. *Journal of Sound and Vibration*, **270**, 427–432 (2004)

[13] Cveticanin, L. Vibrations of the nonlinear oscillator with quadratic nonlinearity. *Physica A*, **341**, 123–135 (2004)

[14] Wu, B. S. and Lim, C. W. Large amplitude nonlinear oscillations of a general conservative system. *International Journal of Non-Linear Mechanics*, **39**, 859–870 (2004)

[15] Hu, H. Exact solution of a quadratic nonlinear oscillator. *Journal of Sound and Vibration*, **295**, 450–457 (2006)

[16] Hu, H. Solution of a quadratic nonlinear oscillator by the method of harmonic balance. *Journal of Sound and Vibration*, **293**, 462–468 (2006)

[17] Hu, H. Solutions of a quadratic nonlinear oscillator: iteration procedure. *Journal of Sound and Vibration*, **298**, 1159–1165 (2006)

[18] Thompson, J. M. T. and Hunt, G. W. *A General Theory of Elastic Stability*, Wiley, London (1973)

[19] Jiang, W. A. and Chen, L. Q. Snap-through piezoelectric energy harvesting. *Journal of Sound and Vibration*, **333**, 4314–4325 (2014)